Physical Chemistry of Freezing Atmospheric Aqueous Drops

Article *in* The Journal of Physical Chemistry A · April 2017

DOI: 10.1021/acs.jpca.7b02571

2 authors:

Anatoli Bogdan
University of Helsinki
59 PUBLICATIONS **544** CITATIONS
SEE PROFILE

Mario J Molina
University of California, San Diego
245 PUBLICATIONS **30,783** CITATIONS
SEE PROFILE

THE JOURNAL OF PHYSICAL CHEMISTRY A

Article

pubs.acs.org/JPCA

Physical Chemistry of the Freezing Process of Atmospheric Aqueous Drops

Anatoli Bogdan*,†,‡ and Mario J. Molina§

†Laboratory of Polymer Chemistry, Department of Chemistry, University of Helsinki, P.O. Box 55, FI-00014 Helsinki, Finland

‡Department of Physics, University of Helsinki, P.O. Box 48, FI-00014 Helsinki, Finland

§Department of Chemistry and Biochemistry, University of California, San Diego, La Jolla, California 92093-0356, United States

Supporting Information

ABSTRACT: In supercooled aqueous solutions, ice nucleation is the initial stage of the freezing process. In this paper, we present experimental results that indicate that during the freezing of aqueous solutions, freeze-induced phase separation (FIPS) into pure ice and a freeze-concentrated solution (FCS) takes place. Our observations involve the use of an optical cryo-microscope (OC-M) to record images and movies. The results visually indicate for the first time that there are two freezing processes for $(NH_4)_3H(SO_4)_2/H_2O$ solutions: (i) contact freezing, as is the case for pure water drops, and (ii) the Wegener−Bergeron−Findeisen process, which is the growth of frozen drops (ice) at the expense of liquid ones. We also present OC-M images of frozen micrometer-scaled H_2SO_4/H_2O drops that support our previous finding that freezing of these solutions generates mixed-phase particles, namely an ice core coated with a FCS. These results are relevant for atmospheric as well as for pharmaceutical sciences.

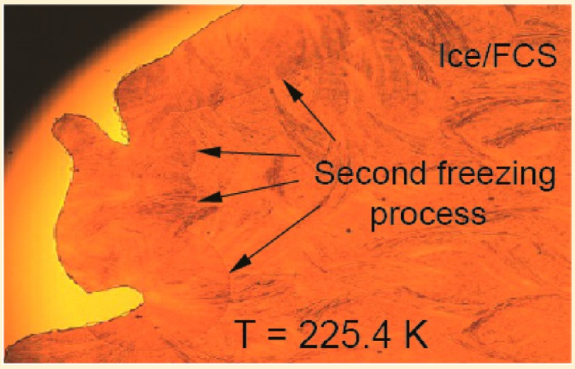

1. INTRODUCTION

High-altitude ice clouds—upper tropospheric (UT) cirrus and ice polar stratospheric clouds (type II ice PSCs)—can be formed by freezing atmospheric aqueous drops that contain an H_2SO_4 and HNO_3 mass fraction up to ∼30 wt %.[1−5] There are reports that UT aqueous drops can contain also a mass fraction of sulfate/organics mixture larger than 50 wt %.[6] It is important to understand what happens to solutes during the freezing of atmospheric aqueous drops and whether they impact the microphysics and the development of high-altitude ice clouds.[1−5]

Regarding the freezing of aqueous solutions, the following are well-known facts: ice is highly intolerant to impurities[7] and, consequently, the expulsion of solute molecules and ions from the forming ice lattice is induced by the freezing process, that is, a freeze-induced phase separation (FIPS) into pure ice and a freeze-concentrated solution (FCS) takes place.[8−11] FIPS occurs not only during freezing upon cooling, but also during freezing upon warming.[12] FIPS and the ice/FCS morphology of frozen solutions is readily observable. OC-M images and movies obtained *in situ* during the freezing of aqueous solutions were presented in our previous work.[5,13−17] FIPS occurs independently of whether the freezing of aqueous solutions has been initiated by homogeneous[1,3−5,8,17] or by heterogeneous[18] ice nucleation. Existing experimental techniques do not distinguish whether FIPS occurs already during ice nucleation in a *uniform* solution, or an ice nucleation event takes place in pure water domains[8,19] within solutions.

FIPS is a well-known phenomenon in medicine, biology, cryobiology, food industry, pharmaceutics, biotechnology, tissue engineering, etc. (refs 13−15 and citations therein). We reported in the past that FIPS takes place also during the freezing of atmospheric aqueous drops—the precursors of UT cirrus[1−4] and ice PSCs[5] and, hence, that, in the atmosphere, FIPS produces mixed-phase cloud particles, namely an ice core enveloped with a FCS coating, and not pure ice crystals. We believe that this coating impacts the pace of development of high-altitude ice clouds, as well as their radiative, physical, and chemical properties. Consequently, we conclude that models of the Earth's climate should take into account the likely mechanism of these freezing events.[1−5,17] Additional insights into high-altitude ice cloud formation under atmospheric conditions can be gained by considering the entire freezing process of atmospheric aqueous drops, and not only the act of ice nucleation. In this paper, we present additional experimental results obtained with OC-M and differential scanning calorimetry (DSC) that further support our earlier conclusions.

2. EXPERIMENTAL SECTION

In this work, we investigated the freezing behavior of (i) emulsified pure water and emulsified H_2SO_4/H_2O solutions, (ii) micrometer-scaled pure water drops nebulized on a silicon

Received: March 18, 2017
Revised: April 9, 2017
Published: April 10, 2017

DOI: 10.1021/acs.jpca.7b02571
J. Phys. Chem. A XXXX, XXX, XXX−XXX

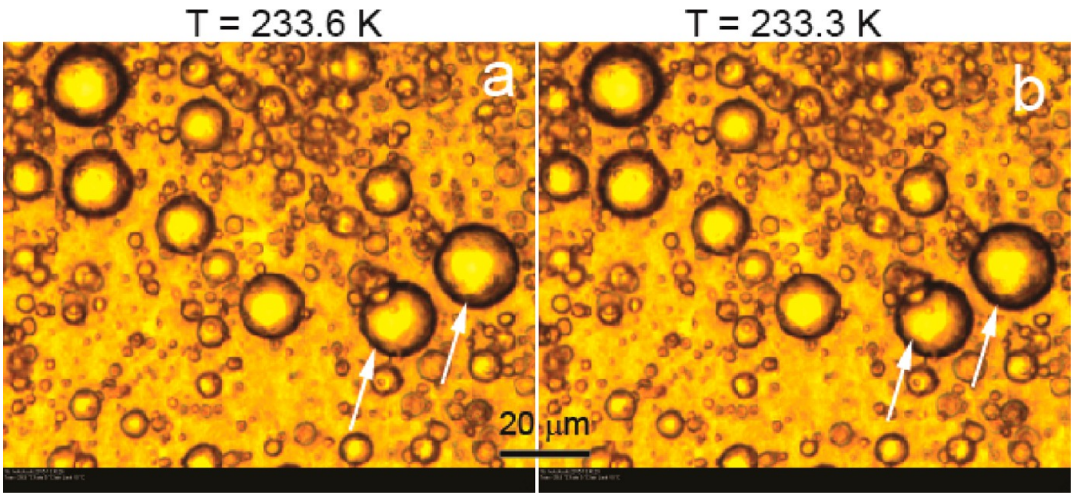

Figure 1. OC-M images taken upon cooling of emulsified pure water drops. The arrows show two drops before freezing (a) and after freezing (b). The scale bar of 20 μm is related to both images. The emulsion sample is cooled at 5 K/min. Note that the size of the outer dark ring increases upon freezing.

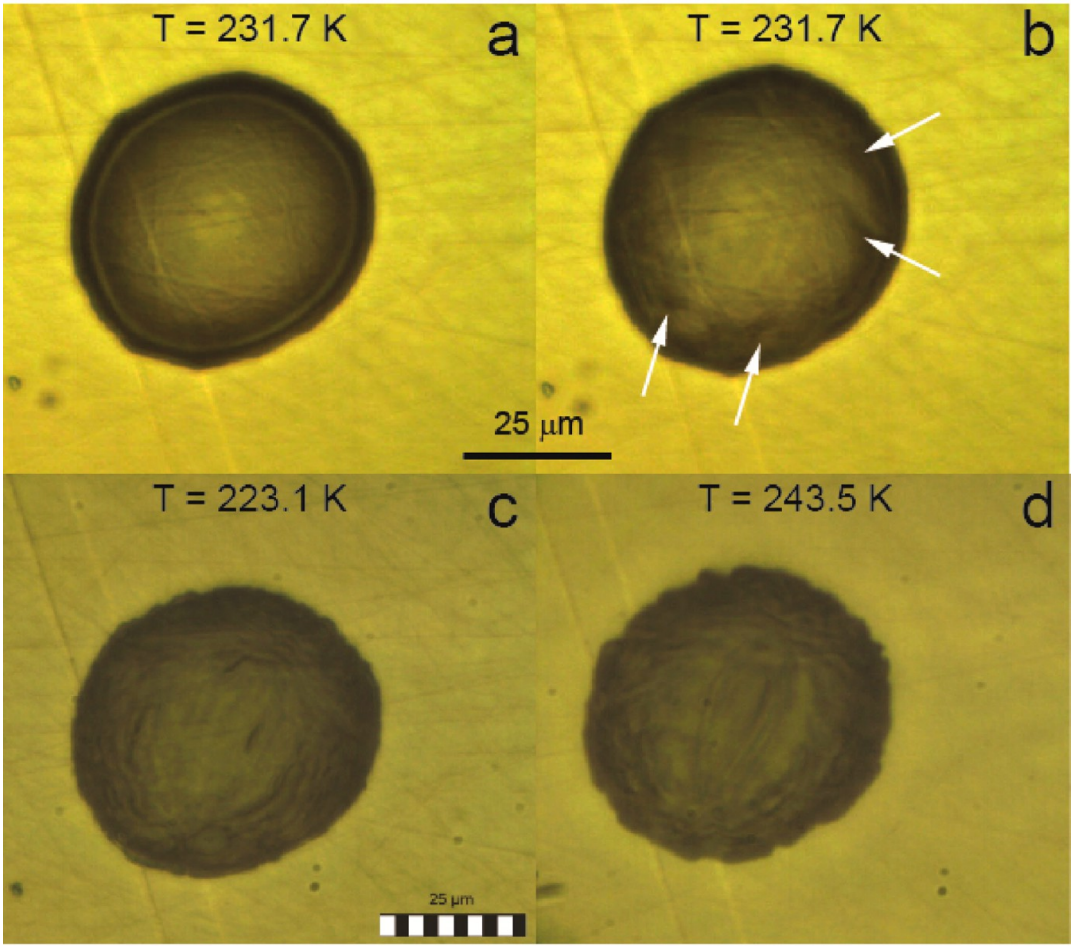

Figure 2. OC-M images of a single pure water drop placed on a Si wafer. Images in parts a and b were taken before and after freezing, respectively. The arrows mark the spots of the ice surface which differ from the surface of the unfrozen drop. The image in part c was taken upon further cooling, and images in part d upon subsequent warming. The drop is cooled and warmed at 3 K/min.

(Si) wafer, and (iii) bulk inorganic and organic solutions relevant to atmospheric and pharmaceutical sciences. Details about solution preparation and emulsification procedure have been described elsewhere.[3−5] For the *in situ* visualization of freezing process and the ice/FCS morphology of frozen solutions we used the ´2-dimensionaĺ solution approach described earlier, employing an Olympus BX51 optical cryo-microscope (OC-M) equipped with a Linkam cold stage and Linksys32 temperature control and video capture software.[13−16] To this end we placed bulk pure water, solution and emulsion

DOI: 10.1021/acs.jpca.7b02571
J. Phys. Chem. A XXXX, XXX, XXX−XXX

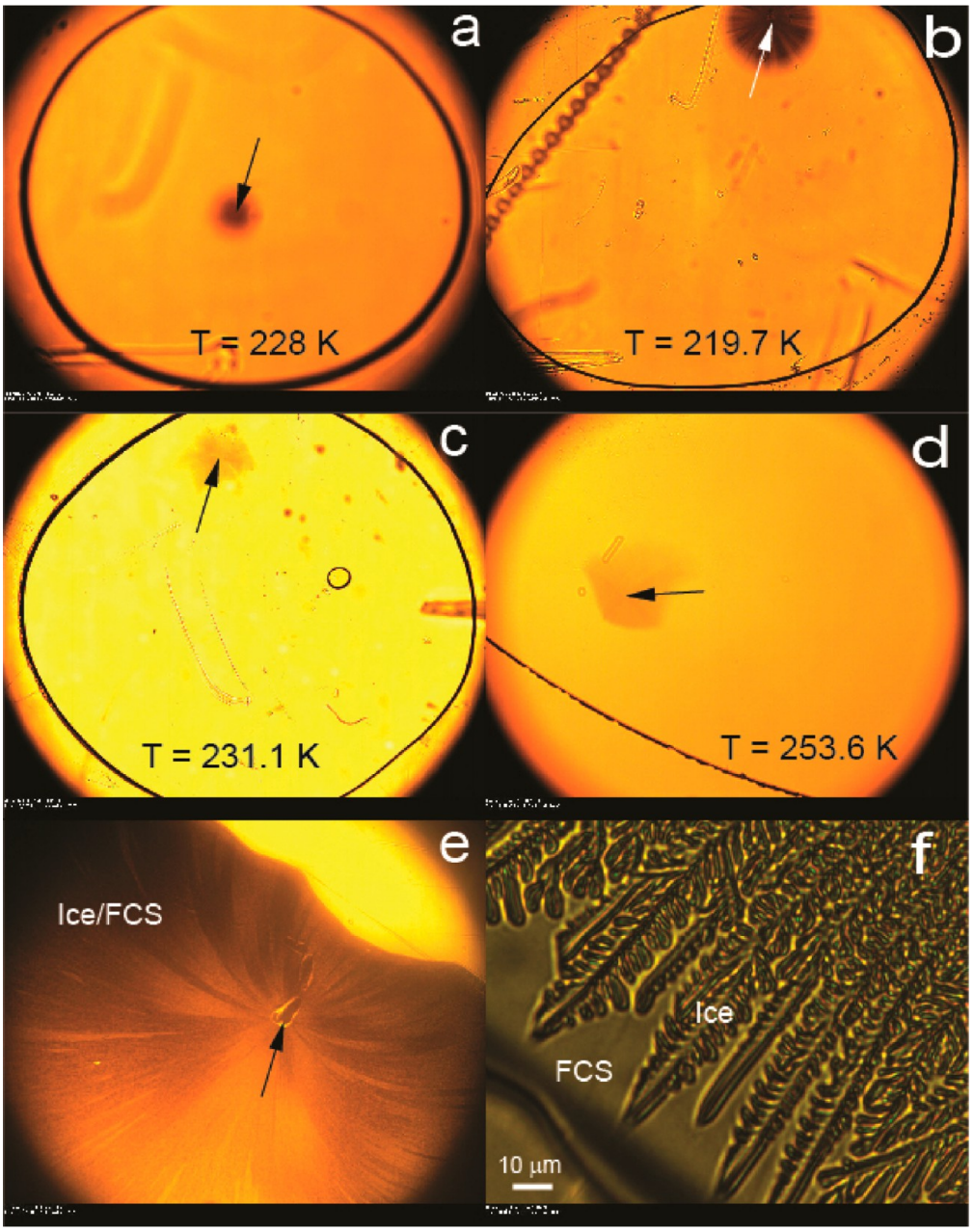

Figure 3. OC-M images in parts a–d demonstrate the onset of freezing upon cooling of four pharmaceutical formulations (see text). Arrows mark the spots of ice nucleation. Images in parts e and f were taken from the fifth formulation after freezing. The arrow in part e marks the spot of heterogeneous ice nucleation. The image in part f shows IF/FCS morphology (see text). All formulations are cooled at 2 K/min.

samples between a microscope glass slide and a cover glass. We also investigated the freezing behavior of bulk pure water and solutions samples (~6 mg) calorimetrically using a Mettler Toledo DSC 822. Details about DSC and OC-M measurements have been described elsewhere.[1−5,8,12−15,18]

3. RESULTS AND DISCUSSION

3.1. OC-M and DSC Measurements. *3.1.1. Freezing Pure Water Drops.* Figure 1 displays two successive OC-M images from Supporting Movie SM1, which was recorded *in situ* during the freezing of emulsified pure water. The SM1 movie is presented in the Supporting Information. In Figures 1a and 1b, arrows mark two drops before freezing and after freezing, respectively. In Figure 1b, the remaining drops are still unfrozen. It can be seen that the OC-M images do not distinguish between liquid and frozen drops. However, the freezing of drops is clearly observable in Movie SM1 as an abrupt increase of drop volume brought about by the reduction of density during water−ice transformation. It is known that the density of ice is ~9% smaller than that of liquid water.[20]

In Figure 2, we present four OC-M images obtained during the cooling and warming of a single pure water drop of diameter ~40 μm placed on a Si wafer. Two successive images in Figures 2a and 2b are selected from Movie SM2, the movie that recorded the freezing of the drop. These images demonstrate that (i) freezing does not convert the drop into a faceted ice crystal, and (ii) the surface of the frozen drop or ice surface is practically as smooth as the surface of the liquid drop. The ice surface becomes rough with time owing to water vapor deposition, as demonstrated by an image taken upon

DOI: 10.1021/acs.jpca.7b02571
J. Phys. Chem. A XXXX, XXX, XXX−XXX

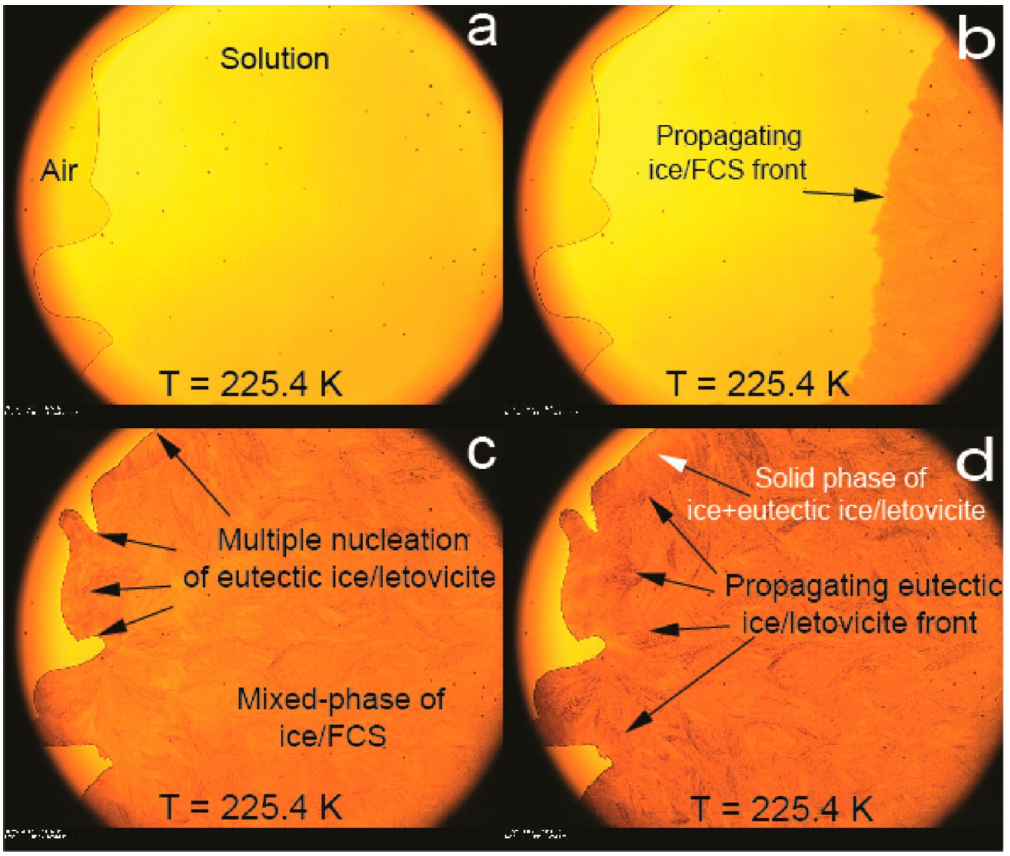

Figure 4. doublé freezing of 35 wt % $(NH_4)_3H(SO_4)_2$. The image in part a is taken from an unfrozen solution. The image in part b is a snapshot of the propagation of the ice/FCS front. In part c, the arrows mark nucleation events of eutectic ice/$(NH_4)_3H(SO_4)_2$ in mixed-phase ice/FCS. The arrows in part d mark the line of the propagation of the eutectic ice/$(NH_4)_3H(SO_4)_2$ front. Note that all processes occur practically at the same temperature, 225.4 K. The cooling rate is 3 K/min.

further cooling (Figure 2c), and by an image taken upon subsequent warming (Figure 2d). Similar "smooth-rough" ice surface transformations were observed during numerous OC-M freezing experiments of pure water drops nebulized on a Si wafer. The rate of change of the ice surface roughness increases with increasing relative humidity.

Movie SM3 was recorded during the freezing of a population of pure water drops of ~10−30 μm in diameter, nebulized on a Si wafer. Images a and b in Figure 2 and Movie SM3 suggest that freezing of almost pure atmospheric water drops, which may be encountered at lower altitudes in troposphere, do not produce faceted ice crystals. The frozen atmospheric drops will transform into faceted ice crystals with time due to vapor deposition, as is demonstrated by the images 2c and 2d and SM3.

The movie SM3 also visually demonstrates (i) the contact freezing mechanism when freezing is initiated by the contact of ice crystals with liquid drops and (ii) the Wegener−Bergeron−Findeisen process, which is the growth of frozen drops (ice) at the expense of liquid ones. In the atmosphere, besides ice crystals, the contact freezing mechanism can be initiated by any solid particles capable to nucleate ice heterogeneously.[21] Although the contact freezing mechanism and the Wegener−Bergeron−Findeisen process are well-known, their explicit visual demonstration is presented here, to our best knowledge, for the first time.

The images in Figures 1 and 2 show that the freezing of pure water drops occurs at 233.3 and 231.7 K, respectively. This fact is surprising, because the drops are large (~10−30 μm in diameter), and are surrounded by an oil-surfactant matrix, or else are in contact with the Si wafer surface. The drops nevertheless freeze within the homogeneous freezing temperature region of ~234−229 K. For comparison, our previous DSC measurements showed that bulk pure water drops of mass ~5−11 mg placed on different substrates froze heterogeneously around ~252 K (see Figure 4 in ref 18).

Finally, we could neither detect ice nucleation events (or the onset of freezing) in our OC-M freezing measurements of (i) micrometer-scaled pure water drops in emulsions (Figure 1), (ii) micrometer-scaled pure water drops nebulized on a Si wafer (Figure 2), and (iii) bulk pure water samples placed in between a glass slide and a cover glass, i.e., ~10−15 μm thick pure water films (not shown). In the first two cases, when entire drops are under observation, the whole freezing process (i.e., ice nucleation event and subsequent ice growth) is practically instantaneous. In the third case, although the whole freezing process is longer because of the much larger sample mass and surface, the difficulty to detect the spot of the onset of freezing (ice nucleation) is due to the fact that a thin layer of pure water and ice are practically indistinguishable in optical microscopy. For example, images in parts a and b of Figure 2 demonstrate that the liquid and frozen drops of thickness ~20 μm are similarly transparent.

3.1.2. Freezing Pharmaceutical Formulations. In contrast to pure water, ice nucleation events or the onset of freezing is detectable in pharmaceutical formulation/solution films placed

DOI: 10.1021/acs.jpca.7b02571
J. Phys. Chem. A XXXX, XXX, XXX−XXX

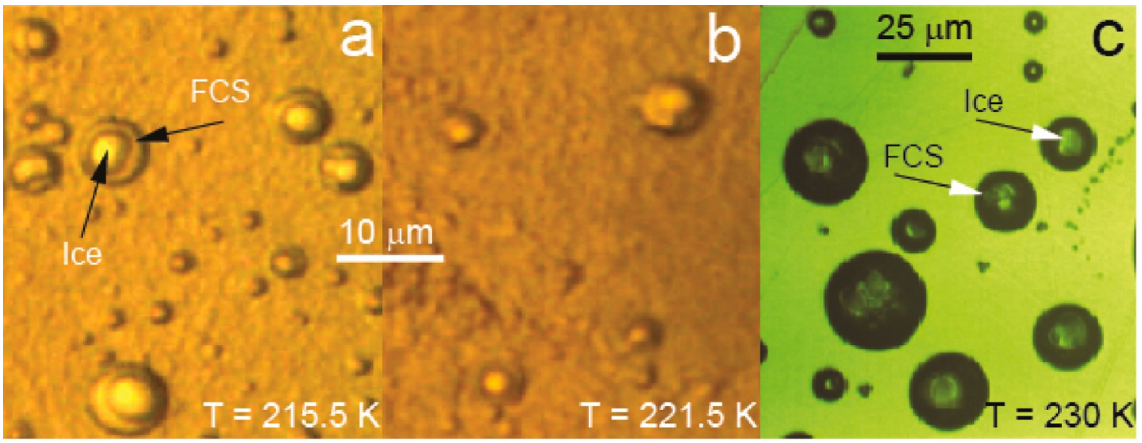

Figure 5. OC-M images of mixed-phase particles formed after the freezing of emulsified 25 wt % H_2SO_4 (a, b) and 15 wt % H_2SO_4 drops placed on a Si wafer (c). Arrows mark an ice core and a FCS coating, respectively.

between a glass slide and a cover glass, as is demonstrated in Figure 3. In these formulations, the citric acid (CA) buffer and the active protein are of different mass ratio with the total concentration of ~30 wt % (CA + protein). Images in parts a-d of Figure 3 were extracted from Movies SM4–SM7 recorded during the freezing of four different formulations. Although the formulations froze very rapidly and ice nucleation occurred often outside the region observable with our microscope, we nevertheless managed to detect several onsets of freezing. The onset of freezing is observed as an *abrupt* black flash in films thicker than ~100 μm (images in Figure 3, parts a and b), and an *abrupt* darkening in ~10–15 μm-thick films (images in Figure 3, parts c and d). The abrupt black flash and darkening are due to light scattering from a rapidly forming complex and ramified spherulitic ice framework (IF), entangled with a FCS.[13−16] The very fast freezing process displayed in Movies SM4–SM7 indicates that ice nucleation and subsequent freezing/ice-growth belong to only one physical process, and, consequently, ice nucleation should be considered together with the entire freezing process. On the other hand, images a–d do not provide information whether the ice nucleation event took place in a uniform solution or in a pure water domain within solutions. As we mentioned in the Introduction, the current experimental techniques do not allow us to observe this behavior *in situ*. Future investigations performed with other experimental techniques may elucidate this matter.

The images in parts e and f of Figure 3 were obtained from the fifth frozen formulation. The arrow in Figure 3e shows the spot of heterogeneous ice nucleation from which a spherulitic IF developed. All images in Figure 3 indicate that in frozen formulations, the ice phase is not a population of isolated ice crystals surrounded by a FCS, as previously believed, but a continuous ramified IF entangled with a FCS.[13−16] In lyophilization/freeze-drying, freezing is the first and most important step. Finding the means to control the pace of FIPS, and, consequently, the morphology of IF/FCS is important for the optimization of time- and energy-consumed lyophilization, which is widely used in pharmaceutics, biotechnology, food industry, tissue engineering, etc.[13−16] The IF/FCS morphology of frozen formulations controls the duration of lyophilization and, consequently, the quality attributes of lyophilized products (drugs, foods, etc.).

3.1.3. Freezing of Aqueous Solutions Relevant to the Atmosphere. In Figure 4, we present OC-M images extracted from Movie SM8, which demonstrate the "double" freezing of 35 wt % $(NH_4)_3H(SO_4)_2$ (letovicite). In the atmosphere, $(NH_4)_3H(SO_4)_2$ is believed to play an important role in the formation of cirrus ice clouds. To our best knowledge, Figure 4 and Movie SM8 present the first visualization evidence of two freezing events/processes. Earlier we reported the occurrence of two and three freezing and melting events,[1,3,4,8,18] and single freezing and triple melting events[22] detected calorimetrically. We also reported two freezing events observed upon warming above the glass transition of $HNO_3/H_2SO_4/H_2O$ and HCl/H_2O.[12] The image in Figure 4a is taken from an unfrozen solution. The first freezing event is due to the freezing of pure ice. The image in Figure 4b shows a snapshot of the propagation of ice/FCS (i.e., IF/FCS) front. The movie SM8 indicates how the propagating ice/FCS front pushes ahead the unfrozen solution, whose movement changes the configuration of the air/solution interface line (compare images in Figures 4, parts b and c). The comparison of images in parts b and c of Figure 4 also shows that the mixed-phase region of ice/FCS becomes darker as the IF develops. The second freezing process is due to the crystallization of eutectic ice/$(NH_4)_3H(SO_4)_2$ within FCS. The image in Figure 4c shows that the crystallization of eutectic ice/$(NH_4)_3H(SO_4)_2$ is initiated from multiple nucleation events. The image in Figure 4d shows a snapshot of the propagation of several eutectic ice/$(NH_4)_3H(SO_4)_2$ fronts. The frozen solution is completely solid after the second freezing event and is composed of ice and eutectic ice/$(NH_4)_3H(SO_4)_2$ (the white arrow in Figure 4d). The two freezing events can be clearly observed in Movie SM8; this movie also indicates that the crystallization of eutectic ice/$(NH_4)_3H(SO_4)_2$ begins after the completion of the freezing of pure ice and that it is much slower than the crystallization of pure ice during the first freezing event.

Image f in Figure 3 (section 3.1.2) shows the approximate dimensions of crystalline ice branches/twigs which make up the IF of a frozen pharmaceutical formulation. Similar dimensions of ice branches/twigs can be observed also in images obtained from the frozen solutions of atmospheric relevance. Judging from the thickness of the ice branches/twigs, one may assume that the frozen drops of diameter less than ~3–5 μm would possess a simpler ice/FCS morphology. Figure 5 shows the images of frozen micrometer-scaled 25 wt % H_2SO_4 emulsified drops (Figure 5, parts a and b), and 15 wt % H_2SO_4 drops nebulized on a Si wafer (Figure 5c). Upper tropospheric

DOI: 10.1021/acs.jpca.7b02571
J. Phys. Chem. A XXXX, XXX, XXX–XXX

aqueous drops can possess a similar concentration.[3,4] The figures and movies indicate that frozen drops are composed of an ice core enveloped with a FCS. These images support our previous works, in which we reported that freezing of atmospheric aqueous drops can produce mixed-phase cloud particles, namely an ice core coated with a FCS.[1−5,17]

3.1.4. DSC Measurements. Figure 6 displays DSC thermograms obtained during the cooling/warming of bulk pure water,

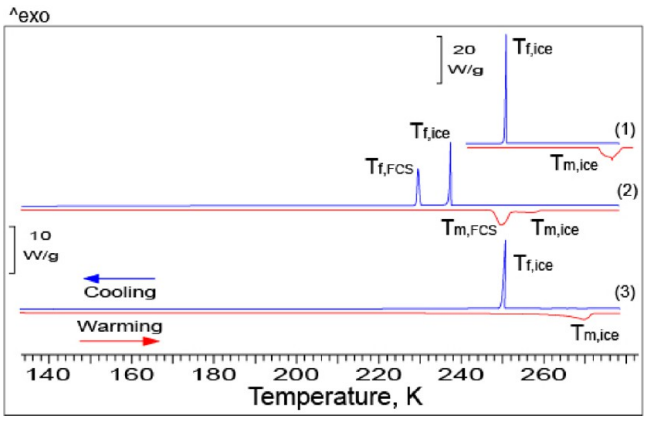

Figure 6. DSC cooling (upper blue curves) and warming (lower red curves) thermograms of bulk pure water (1), 35 wt % $(NH_4)_3H(SO_4)_2$ (2) and ∼30 wt % (CA + protein) formulation (3). Exothermic peaks $T_{f,ice}$ and $T_{f,FCS}$ are due to the freezing out of pure ice and the crystallization of eutectic ice/$(NH_4)_3H(SO_4)_2$, respectively. The endothermic peaks $T_{m,ice}$ and $T_{m,FCS}$ are due to the melting of ice and eutectic ice/$(NH_4)_3H(SO_4)_2$, respectively. The mass of all the DSC samples is ∼6 mg. The cooling and warming rate of all samples is 3 K/min. The two scale bars indicate heat flow through the samples.

35 wt % $(NH_4)_3H(SO_4)_2$ solution and ∼30 wt % (CA + protein) formulation. The analysis of the DSC thermograms, together with the OC-M images/movies obtained from the same solutions, provides information about the freezing behavior, which cannot be gained when DSC and OC-M are used separately. Figure 6 shows that pure water produces one exothermic ice freezing peak $T_{f,ice}$ and one endothermic ice melting peak $T_{m,ice}$. Unlike pure water, bulk 35 wt % $(NH_4)_3H(SO_4)_2$ produces two freezing, $T_{f,ice}$ and $T_{f,FCS}$, and two melting, $T_{m,ice}$ and $T_{m,FCS}$, peaks. According to Movie SM8, the peak $T_{f,ice}$ is due to the freezing out of pure ice. The peak $T_{f,FCS}$ is due to the crystallization of eutectic ice/$(NH_4)_3H(SO_4)_2$ from FCS (see also Figure 4). The two melting processes $T_{m,FCS}$ and $T_{m,ice}$ are due to the melting of eutectic ice/$(NH_4)_3H(SO_4)_2$ and ice, respectively. However, in contrast to Movie SM8, which demonstrates that the second freezing event $T_{f,FCS}$ begins right away after the completion of freezing out of pure ice, in Figure 6 the two freezing events of $T_{f,ice}$ and $T_{f,FCS}$ are separated by the temperature interval of ∼6 K, that is, a time of ∼2 min. This temperature/time separation between $T_{f,ice}$ and $T_{f,FCS}$ can be accounted for by the dependence of $T_{f,ice}$ on the size or, in our case, on the thickness of $(NH_4)_3H(SO_4)_2/H_2O$ sample. It is a well-known experimental fact that $T_{f,ice}$ decreases with size. In contrast, $T_{f,FCS}$ most likely occupies a relatively narrow temperature region similar to that which we observed for the bulk $(NH_4)_2SO_4/H_2O$ solutions (see Figure 1 in ref 18.).

Further, the thermograms of bulk ∼30 wt % (CA + protein) do not show any indication of the second freezing and melting events (Figure 6). However, the magnification of these thermograms reveals two liquid-glass and two reverse glass−liquid transitions that occur below $T_{f,ice}$ (not shown). The appearance of these two glass transitions is similar to the appearance of the two glass transitions that we observed in the cooling/warming thermograms of aqueous citric acid and sucrose.[13,14] We reported that these two glass transitions are produced by the two freeze-concentrated solutions, FCS_1 and FCS_2, of different concentrations.[13,14] Most likely, in our case, the two transitions of ∼30 wt % (CA + protein) can also be produced by two FCS_1 and FCS_2, of different concentrations.

3.1.5. Freezing Rate. Intuitively, in pure water, the freezing rate may be viewed as the pace of rearrangement of H_2O molecules from liquid to solid/ice state. In aqueous solutions, the freezing rate may differ from that in pure water because of FIPS, i.e., because of the expulsion of solute molecules and ions from the ice lattice during the freezing of pure ice. For example, Movies SM1−SM3 show that micrometer-scaled supercooled pure water drops freeze practically instantaneously. Movie SM8 shows that the freezing of pure ice in 35 wt % $(NH_4)_3H(SO_4)_2$ is much slower, despite its supercooling being as much as ∼6 K larger than that of pure water drops. These observations suggest that the pace of the freezing process in pure water and aqueous solutions is different. In OC-M measurements, the freezing rate may be defined as the pace of the propagation of the ice−water or ice/FCS front. However, such definition depends on the supercooling and thickness of the water/aqueous films.

Below we show that freezing rate can be approximately determined using stretched freezing peaks $T_{f,ice}$ taken from Figure 6, but reduced to a single vertical scale, as is demonstrated in Figure 7. It can be observed that the steepness

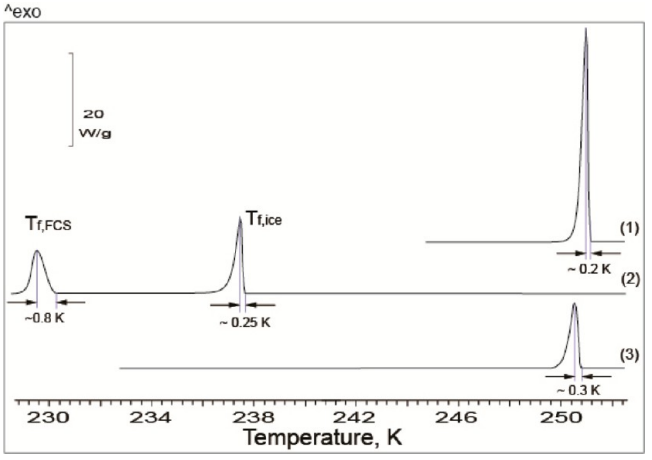

Figure 7. Stretched freezing peaks in cooling thermograms taken from Figure 6.

of the peaks $T_{f,ice}$—the temperature region from the onset of freezing to the maximum peak height—is different. The steepness of peak $T_{f,ice}$ characterizes how fast the enthalpy of fusion evolves during ice crystallization and is withdrawn by the applied cooling rate. On the other hand, it is a well-known experimental fact that in the freezing experiments on supercooled aqueous samples, which are not subjected to a cooling rate, the evolved enthalpy of fusion rapidly rises the temperature of the sample to ∼273 K. In our case, the time of freezing can be estimated from the peak steepness and the applied cooling rate of 3 K/min. Calculation gives ∼4, 5, and 6 s for pure water, 35 wt % $(NH_4)_3H(SO_4)_2$ and ∼30 wt % (CA + protein), respectively. For comparison, at a similar cooling

DOI: 10.1021/acs.jpca.7b02571
J. Phys. Chem. A XXXX, XXX, XXX−XXX

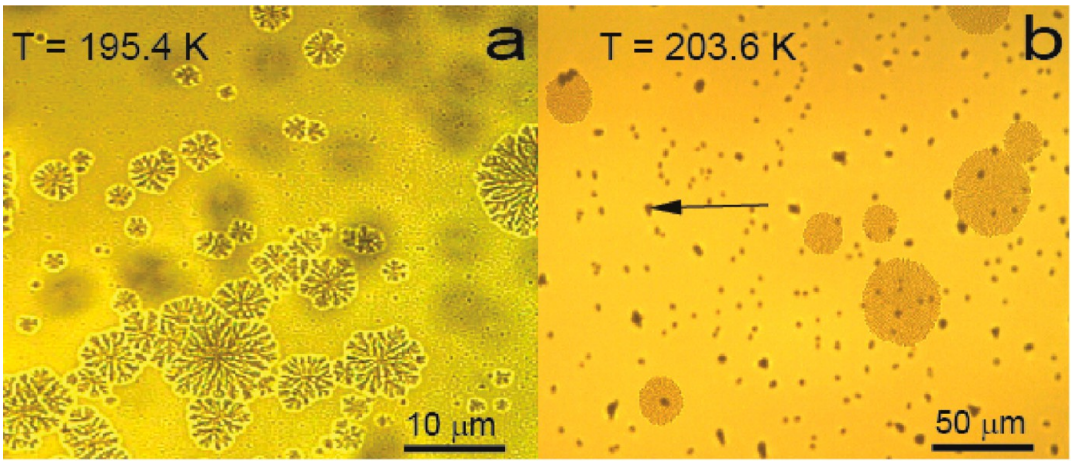

Figure 8. Multiple ice nucleation events in highly concentrated sucrose/H_2O (a) and CA/H_2O (b). In part b, numerous small dark spots (one is marked by an arrow) are ice crystals formed by vapor deposition on the cover glass. Cooling rate is 5 K/min.

rate, the freezing time of pure water and 35 wt % $(NH_4)_3H(SO_4)_2$ drops of 1 μm in diameter would be ~0.0003 and 0.0004 s, respectively. These values give an insight into the freezing time of atmospheric aqueous drops which are usually subjected to cooling rates smaller than 80 K/h.[3]

Further, all DSC samples possess a similar mass of ~6 mg. Consequently, in 35 wt % $(NH_4)_3H(SO_4)_2$ and ~30 wt % (CA + protein) samples, the mass of water is ~3.9 and 4.2 mg of H_2O, respectively. However, not all this liquid water transforms to ice at $T_{f,ice}$. A fraction of water remains unfrozen in a FCS. Assuming that in both samples about 3 mg of H_2O transforms to ice at $T_{f,ice}$, we estimate the freezing rate as the pace of the enthalpy of fusion evolved (i) per unit time and (ii) per K for bulk pure water, 35 wt % $(NH_4)_3H(SO_4)_2$, and ~30 wt % (CA + protein). We obtain the following pairs of values: (11.8 and 236), (6.9 and 138) and (4.8 and 95) with the dimensions of W/g·s and W/g·K, respectively. These values indicate that (i) the solutes reduce the freezing rate in comparison with that of pure water, and (ii) the freezing rate is smaller in solutions containing solutes of complex molecular structure. In other words, the freezing rate and, consequently, the pace of the expulsion of solute molecules and ions from the ice lattice (i.e., FIPS) decreases with increasing solute concentration and with the complexity of the molecular structure of the solutes, i.e., with increasing viscosity. We anticipate that, with further elaboration, the proposed above semiquantitative description of the freezing rate can be used for the appropriate definition of freezing rate for the characterization of freezing aqueous solutions or pharmaceutical formulations.

In Figure 7, the steep warm side of $T_{f,ice}$ peaks indicates that the freezing out of pure ice is initiated from a single nucleation event. This is confirmed by Movies SM4–SM8, which indicate a rapid freezing process. In contrast, the warm side of the $T_{f,FCS}$ peak is not steep. Figure 4 and Movie SM8 indicate that the crystallization of eutectic ice/$(NH_4)_3H(SO_4)_2$ starts from multiple nucleation events. An increase in the number of nucleation events is brought about by increasing viscosity, because it slows down the crystallization of eutectic ice/$(NH_4)_3H(SO_4)_2$. Figure 8 shows that the number of ice nucleation events increases as well with concentration. As the temperature decreases further, the growth of numerous ice crystals is terminated by the glass transition of a FCS formed around these ice crystals. The terminated freezing process would resume upon subsequent warming above a reverse glass–liquid transition.[13,14] Figure 8 may be considered as a visual argument that indicates that consideration of ice nucleation by itself does not give the complete physical picture of the freezing phenomenon; subsequent ice crystallization should be considered as well.

In summary, although the freezing rate of aqueous solutions can be controlled by concentration, and, to a lesser degree by the molecular structure of the solute(s), we conclude that, independently of which solid is going to be formed (ice or eutectic ice/letovicite), a nucleation event is only the onset of the freezing process.

4. CONCLUSIONS

We have presented visualization evidence of FIPS into pure ice and a FCS, which occurs during the freezing of aqueous solutions relevant to atmospheric and pharmaceutical sciences. We have also presented to our best knowledge, for the first-time, visualization evidence of two freezing events of $(NH_4)_3H(SO_4)_2/H_2O$ solutions, and the visual demonstration of a contact-freezing mechanism during the freezing of micrometer-scaled pure water drops, and the Wegener–Bergeron–Findeisen process, that consists of the growth of ice drops at the expense of the liquid solution. Furthermore, we have presented visualization evidence indicating that micrometer-scaled pure water drops remain practically spherical after freezing, with a smooth ice surface. The spherical frozen drops convert to faceted ice crystals with time, due to vapor deposition. Our movies obtained *in situ* during the freezing of aqueous solutions indicate that ice nucleation is only the onset of the freezing process, and, consequently, cannot be considered separately from the whole freezing process of aqueous drops. The OC-M measurements presented here support our previous DSC findings that freezing atmospheric drops produce mixed-phase cloud particles, namely an ice core coated with a FCS.[1−5,17]

■ ASSOCIATED CONTENT

Supporting Information

The Supporting Information is available free of charge on the ACS Publications website at DOI: 10.1021/acs.jpca.7b02571.

Captions for the movies references in this paper (PDF)

DOI: 10.1021/acs.jpca.7b02571
J. Phys. Chem. A XXXX, XXX, XXX−XXX

Movie SM1. Freezing of emulsified pure water drops (AVI)
Movie SM2: Freezing of a single pure water drop (AVI)
Movie SM3: Freezing of population of pure water drops placed on a Si wafer (AVI)
Movie SM4: Freezing of pharmaceutical formulation 1 (AVI)
Movie SM5: Freezing of pharmaceutical formulation 2 (AVI)
Movie SM6: Freezing of pharmaceutical formulation 3 (AVI)
Movie SM7: Freezing of pharmaceutical formulation 4 (AVI)
Movie SM8: Double freezing of aqueous letovicite (AVI)

AUTHOR INFORMATION

Corresponding Author

*(A.B.) E-mail: anatoli.bogdan@helsinki.fi.

ORCID

Anatoli Bogdan: 0000-0001-7339-6673

Notes

The authors declare no competing financial interest.

ACKNOWLEDGMENTS

A.B. thanks the Department of Chemistry, University of Helsinki (Finland), for using DSC, University of Innsbruck (Austria) for using OC-M, and S. Aichholzer from Arbeitsmarktservice (AMS, Innsbruck) for her professional behavior and attitude. A.B. did not receive any financial support from funding agencies in the public, commercial, or not-for-profit sectors during the accomplishment of this work. Financial support by A.B.'s family is greatly appreciated.

REFERENCES

(1) Bogdan, A.; Molina, M. J.; Sassen, K.; Kulmala, M. Formation of low-temperature cirrus from H_2SO_4/H_2O aerosol droplets. *J. Phys. Chem. A* **2006**, *110*, 12541−12542.

(2) Räisänen, P.; Bogdan, A.; Sassen, K.; Kulmala, M.; Molina, M. J. Impact of H_2SO_4/H_2O coating and ice crystal size on radiative properties of sub-visible cirrus. *Atmos. Chem. Phys.* **2006**, *6*, 4659−4667.

(3) Bogdan, A.; Molina, M. J. Why does large relative humidity with respect to ice persist in cirrus ice clouds? *J. Phys. Chem. A* **2009**, *113*, 14123−14130.

(4) Bogdan, A. Reversible Formation of Glassy Water in Slowly Cooling Diluted Drops. *J. Phys. Chem. B* **2006**, *110*, 12205−12206.

(5) Bogdan, A.; Molina, M. J.; Tenhu, H.; Mayer, E.; Loerting, T. Formation of mixed-phase particles during the freezing of polar stratospheric ice clouds. *Nat. Chem.* **2010**, *2*, 197−201.

(6) Froyd, K. D.; Murphy, D. M.; Sanford, T. J.; Thomson, D. S.; Wilson, J. C.; Pfister, L.; Lait, L. Aerosol composition of the tropical upper troposphere. *Atmos. Chem. Phys.* **2009**, *9*, 4363−4385.

(7) Petrenko, V. F.; Whitworth, R. W. *Physics of Ice*; Oxford University Press: London, U.K., 2002.

(8) Bogdan, A.; Molina, M. J. Aqueous Aerosol May Build Up an Elevated Upper Tropospheric Ice Supersaturation and Form Mixed-Phase Particles after Freezing. *J. Phys. Chem. A* **2010**, *114*, 2821−2829.

(9) Cheng, J.; Soetjipto, C.; Hoffmann, M. R.; Colussi, A. J. Confocal fluorescence microscopy of the morphology and composition of interstitial fluids in freezing electrolyte solutions. *J. Phys. Chem. Lett.* **2010**, *1*, 374−378.

(10) Robinson, C.; Boxe, C. S.; Guzman, M. I.; Colussi, A. J.; Hoffmann, M. R. Acidity of frozen electrolyte solutions. *J. Phys. Chem. B* **2006**, *110*, 7613−7616.

(11) Vrbka, L.; Jungwirth, P. Brine rejection from freezing salt solutions: A molecular dynamics study. *Phys. Rev. Lett.* **2005**, *95*, 148501.

(12) Bogdan, A.; Loerting, T. Phase separation during freezing upon warming of aqueous solutions. *J. Chem. Phys.* **2014**, *141*, 18C533.

(13) Bogdan, A.; Molina, M. J.; Tenhu, H.; Bertel, E.; Bogdan, N.; Loerting, T. Visualization of freezing process in situ upon cooling and warming of aqueous solutions. *Sci. Rep.* **2014**, *4*, 7414.

(14) Bogdan, A.; Molina, M. J.; Tenhu, H.; Loerting, T. Multiple glass transitions and freezing events of aqueous citric acid. *J. Phys. Chem. A* **2015**, *119*, 4515−4523.

(15) Bogdan, A.; Molina, M. J.; Tenhu, H. Freezing and glass transitions upon cooling and warming and ice/freeze-concentrated-solution morphology of emulsified aqueous citric acid. *Eur. J. Pharm. Biopharm.* **2016**, *109*, 49−60.

(16) Bogdan, A.; Molina, M. J.; Tenhu, T. Visualization data on the freezing process of micrometer-scaled aqueous citric acid drops. *Data in Brief* **2017**, *10*, 144−146.

(17) Bogdan, A.; Molina, M. J.; Kulmala, M.; Tenhu, H.; Loerting, T. Solution coating around ice particles of incipient cirrus clouds. *Proc. Natl. Acad. Sci. U. S. A.* **2013**, *110*, E2439.

(18) Bogdan, A.; Loerting, T. Impact of substrate, aging, and size on the two freezing events of $(NH_4)_2SO_4/H_2O$ droplets. *J. Phys. Chem. C* **2011**, *115*, 10682−10693.

(19) Hudait, A.; Molinero, V. Ice crystallization in ultrafine water-salt aerosols: nucleation, ice-solution equilibrium, and internal structure. *J. Am. Chem. Soc.* **2014**, *136*, 8081−8093.

(20) Lide, D. R. *CRC Handbook of Chemistry and Physics*, 86th ed.; CRC Press: Boca Raton, FL, 2005.

(21) Fornea, A.; Brooks, S.; Dooley, J.; Saha, A. Heterogeneous freezing of ice on atmospheric aerosols containing ash, soot, and soil. *J. Geophys. Res.* **2009**, *114* (D13), 201.

(22) Bogdan, A.; Molina, M. J.; Tenhu, H.; Loerting, T. Single freezing and triple melting of micrometer scaled $(NH_4)_2SO_4/H_2O$ droplets. *Phys. Chem. Chem. Phys.* **2011**, *13*, 19704−19706.

DOI: 10.1021/acs.jpca.7b02571
J. Phys. Chem. A XXXX, XXX, XXX−XXX